



LAWRENCE  
LIVERMORE  
NATIONAL  
LABORATORY

# Effect of Solution Annealing Temperatures on the Crevice Corrosion Mode of Alloy 22

B. S. El-Dasher, R. Etien, S. G. Torres

November 3, 2005

Corrosion 2006  
San Diego, CA, United States  
March 12, 2006 through March 16, 2006

## **Disclaimer**

---

This document was prepared as an account of work sponsored by an agency of the United States Government. Neither the United States Government nor the University of California nor any of their employees, makes any warranty, express or implied, or assumes any legal liability or responsibility for the accuracy, completeness, or usefulness of any information, apparatus, product, or process disclosed, or represents that its use would not infringe privately owned rights. Reference herein to any specific commercial product, process, or service by trade name, trademark, manufacturer, or otherwise, does not necessarily constitute or imply its endorsement, recommendation, or favoring by the United States Government or the University of California. The views and opinions of authors expressed herein do not necessarily state or reflect those of the United States Government or the University of California, and shall not be used for advertising or product endorsement purposes.

EFFECT OF SOLUTION ANNEALING TEMPERATURES ON THE CREVICE  
CORROSION MODE OF ALLOY 22

Bassem S. El-Dasher  
Lawrence Livermore National Laboratory  
P.O.Box 808, L-631  
Livermore, CA 94550

Robert A. Etien  
Lawrence Livermore National Laboratory  
P.O.Box 808, L-631  
Livermore, CA 94550

Sharon G. Torres  
Lawrence Livermore National Laboratory  
P.O.Box 808, L-631  
Livermore, CA 94550

**ABSTRACT**

The effect of solution annealing temperature on the observed corrosion attack mode in Alloy 22 welds was assessed. Three types of specimens were examined, including the as-welded state, solution annealed for 20 minutes at 1121°C, and solution annealed for 20 minutes at 1200°C. The microstructures of the specimens were first mapped using electron backscatter diffraction to determine the grain structure evolution due to solution annealing. The specimens were then subjected to electrochemical testing in a 6 molal NaCl + 0.9 molal KNO<sub>3</sub> environment to initiate crevice corrosion. Examination of the specimen surfaces after corrosion testing showed that in the as-welded specimen, corrosion was present in both the weld dendrites as well as around the secondary phases. However, the specimen solution annealed at 1121°C showed corrosion only at secondary phases and the specimen annealed at 1200°C showed pitting corrosion only in a handful of grains.

## INTRODUCTION

Alloy 22 (UNS N06022) is a nickel-based alloy containing approximately 22% chromium, 13% molybdenum, 3% iron, and 3% tungsten. It has been selected as the candidate material for the outer barrier of the nuclear waste containers for the potential repository site at Yucca Mountain, Nevada [1,2] primarily due to its excellent resistance to pitting and crevice corrosion, as well as stress corrosion cracking [3-8]. However, Alloy 22 welds are known to form potentially detrimental tetrahedrally close packed (TCP) phases upon solidification [9]. Previous experiments on Alloy 22 specimens artificially aged at high temperatures have shown a decrease in corrosion performance in hot acidic solutions and a reduction in mechanical properties [10], apparently due to TCP phase formation.

Solution annealing has been traditionally employed to homogenize Alloy 22 and eliminate the TCP phases from solidified microstructures. This is performed at the manufacturer recommended temperature of 1121°C (2050°F) [11]. Studies conducted to determine the effect of solution annealing on the TCP phase stability [12,13] of Alloy 22 welds presented conflicting results for short-term solution annealing durations. However it was evident that longer-term solution anneals [14] do indeed dissolve the TCP phases in the weld, indicating that the solute distribution is becoming more and more homogeneous. Considering that multiple welds are required for the construction of the waste package outer barrier, an understanding of the effect solution annealing on the corrosion behavior of these welds is important.

In this work we present a study in which crevice corrosion tests were performed on Alloy 22 weld specimens at three solution anneal conditions. The first set of specimens studied was in an as-welded (as-received) condition, the second set was solution annealed for 20 minutes at 1121°C, and the third set was solution annealed for 20 minutes at 1200°C. The microstructures of three specimens (one from each set) were examined before and after the crevice corrosion tests in order to correlate the corrosion mode to the grain structure.

## EXPERIMENTAL

Specimens used in this study were cut from a 30" (762mm) long, 1.5" (38.1mm) thick welded plates. The plates were produced by double-U multi-pass gas-tungsten-arc welds fabricated using 1.5" mill annealed Alloy 22 plates and matching Alloy 22 filler wire (ERNiCrMo-10) [15]. All specimens were cut from the same plate to minimize compositional variability between the specimens. Cutting was performed using an abrasive water jet to minimize heat input during the cutting process thereby minimizing any unwanted side effects on the microstructure. The specimens were cut such that they could be setup for corrosion testing as a prism crevice assembly (PCA). The set-up is based on crevice formers described by the American Society for Testing and Materials (ASTM) in ASTM G 48 and G61. Figure 1 shows a typical PCA setup, with the specimen sandwiched between two crevice formers.

Twelve total specimens were produced, with four specimens for each condition (as-welded, annealed at 1121°C, and annealed at 1200°C). Solution annealing was carried out in air-furnaces for 20 minutes at the appropriate temperature, followed by a water quench. Three specimens from each condition were then prepared for electrochemical testing by grinding all sides to 600 grit to ensure comparable electrochemical testing condition. The fourth specimen from each set was polished and set aside for microstructural characterization before and after the testing. For the specimens intended for characterization, three tasks were involved:

1. Determination of microstructure prior to crevice corrosion,
2. Electrochemical testing to initiate crevice corrosion of the specimens, and
3. Characterization of the microstructure after crevice corrosion to compare the corrosion modes of the three specimens.

It was decided to limit the characterization prior to corrosion to half of one side of each prism as this allowed for a representative coverage of all types of areas. However this was still an appreciably large area, and an appropriate technique to map this area was needed. Automated electron backscatter diffraction (EBSD) [16,17] was determined to be the ideal tool for this task, although this required metallographic preparation of the working surfaces of the specimens. This was accomplished by grinding using progressively finer grit down to 1200 grit, and subsequent polishing to 0.02 $\mu\text{m}$  colloidal silica. After polishing, the specimens were sequentially degreased using hexane, acetone and methanol.

The EBSD system employed consisted of a Peltier cooled CCD camera in a scanning electron microscope (SEM). The specimens were tilted to 70° in the SEM chamber, and the electron beam was collimated into a spot (an accelerating voltage of 30kV and a beam current of 98 $\mu\text{A}$  were used for this study). This spot was scanned across each specimen surface in regular steps to form a square grid. At each step, a diffraction pattern was collected and solved to identify the local crystal orientation. The orientation is then saved in the form of three Eulerian angles. At the conclusion of the scan, the resultant data was compiled into a spatial map that is used to display the locations of grains and grain boundaries. Due to the size of the area of interest, a combination of beam and stage translations were used during the scans. Data were collected on a square grid step sizes of 10 $\mu\text{m}$ , and covering an area of approximately 9mm by 20mm.

Electrochemical tests were conducted on the PCA's in an environment of 6 molal NaCl + 0.9 molal KNO<sub>3</sub> at a temperature of 90°C. These consisted of cyclic potentiodynamic polarization (CP) tests starting at approximately 100 mV below the corrosion potential (determined from previous open circuit potential tests). For the nine specimens intended solely for electrochemical testing, this continued until a current density of 5 mAcm<sup>-2</sup> before the scan was reversed, while for the specimens characterized prior to electrochemical testing, this only continued until a current density of 1 mAcm<sup>-2</sup>. This lower maximum current density was used to yield a smaller amount of corrosion, as this allowed us to capture the initial corrosion behavior under the crevice formers.

After the electrochemical tests were completed, the specimens were rinsed and dried. The weld microstructures under the crevice former were then imaged for the three specimens characterized prior to corrosion testing in order to determine their corrosion behavior.

## RESULTS AND DISCUSSION

Typical cyclic polarization curves for the three types of PCA specimens are shown in Figure 2. It can be seen that the general behavior for the three specimens is in general similar, with very similar breakdown and repassivation potentials (all within 100mV of each other).

In Figure 3, the EBSD maps obtained prior to the electrochemical tests are shown as inverse pole figure maps. The colors represent the crystallographic plane normals parallel to the specimen surface normal, and blocks of a single color indicate one grain. It can be clearly seen in Figure 3(a) and (b) that the weld fusion zone runs through the center of the specimens, where the fusion zone dendrites are significantly coarser than those of the base metal on either side. It can also be seen that partial recrystallization of the fusion zone dendrites is taking place in the specimen solution annealed at 1121°C (Figure 3(b), since multiple small grains appear. By contrast however, the specimen solution annealed at 1200°C (Figure 3(c)) shows that full recrystallization of the fusion zone has taken place, with the grain size distribution more homogeneous.

Although the cyclic polarization curves for the three types of microstructures (Figure 2) are similar, the effect of the microstructural changes on the corrosion behavior is markedly different. In Figure 4, the corrosion effects on all three specimens are shown. For the as-welded specimen, the majority of the corrosion is seen in the weld dendrites (Figure 4(a)). The interdendritic regions appear resistant to attack, with the exception of regions directly next to TCP phases in the interdendritic regions. This behavior is expected, as solute segregation during solidification has been known to cause increased amount of Cr and Mo in the interdendritic region. Also, since TCP phases are rich in Cr and Mo, their presence in turn requires the regions around them to be depleted from these elements. Hence the observations in Figure 4(a) and (b) indicate that the heterogeneous Cr and Mo distribution are responsible for the corrosion mode observed.

After annealing at 1121°C for 20 minutes, it is expected that along with recrystallization, the Cr and Mo distribution becomes more homogeneous. It is also anticipated that some of the TCP phases begin dissolving, further increasing the chemical homogeneity of the weld. In Figure 4(c) and (d), it can be seen that material dissolution occurs in the interdendritic regions, specifically at the areas corresponding to TCP phase locations. In the higher magnification image (Figure 4(d)), the microstructure shows TCP phase shaped pits. Due to their high Cr and Mo content however, it is unlikely that the TCP phases themselves were attacked. Rather, it appears that since virtually all the corrosion occurred at the TCP phase/matrix interfaces, the TCP phases fell out of the specimen during the corrosion test. This then indicates that solution annealing at 1121°C for 20 minutes minimizes the likelihood of dendritic corrosion, at the expense of focusing corrosion around the TCP phases which apparently do not have an adequate amount of time to dissolve into the solid solution during the annealing process.

Post-corrosion characterization of the specimen annealed at 1200°C for 20 minutes was somewhat difficult, as only one small area under the crevice showed signs of corrosion. Micrographs for this area are presented in Figures 4(e) and (f), and it can be seen that the corrosion mode is typical of crevice corrosion in wrought materials, with many fine pits seen in multiple grains. Overall, it is apparent from Figure 4 that the specimen annealed at 1200°C had less localized corrosion at the micro-level than the other specimens.

This study then shows that although the overall corrosion behavior as measured using CPP (Figure 2) did not reflect significant changes between the three specimens, the corrosion behaviors at the micro-level were indeed quite different. However to fully ascertain the correspondence between the macro-level observations and micro-level events, further studies are needed.

## SUMMARY

Alloy 22 prototypical thick weld specimens were studied for the effect of solution annealing on the corrosion behavior. Specimens were examined in the as-welded, solution annealed at 1121°C for 20 minutes, and solution at 1200°C for 20 minutes states. Although cyclic polarization tests showed no discernible difference between the corrosion behavior of the three types of specimens, the mode of corrosive attack at the micro-level was vastly different. The as-welded specimens were primarily attacked in the secondary dendrites, and around the secondary phases in the interdendritic region, whereas the specimen annealed at 1121°C showed attack solely around the TCP phases in the interdendritic regions. The specimen annealed at 1200°C was fully recrystallized, and showed pitting in only a few grains, with no apparent pattern or preference (similar to wrought material).

## ACKNOWLEDGMENTS

Michael M. McGregor and Robert G. Erler are gratefully acknowledged for their assistance in sample treatment and preparation. Raul B. Rebak is gratefully acknowledged for discussions. This work was performed under the auspices of the U. S. Department of Energy by the University of California Lawrence Livermore National Laboratory under contract N W-7405-Eng-48. This work is supported by the Office of Civilian Radioactive Waste Management (OCRWM), U.S. Department of Energy.

## DISCLAIMER

This document was prepared as an account of work sponsored by an agency of the United States Government. Neither the United States Government nor the University of California nor any of their employees, makes any warranty, express or implied, or assumes any legal liability or responsibility for the accuracy, completeness, or usefulness of any information, apparatus, product, or process disclosed, or represents that its use would not infringe privately owned rights. Reference herein to any specific commercial product, process, or service by trade name, trademark, manufacturer, or otherwise, does not necessarily constitute or imply its endorsement, recommendation, or favoring by the United States Government or the University of California. The views and opinions of authors expressed herein do not necessarily state or reflect those of the United States Government or the University of California, and shall not be used for advertising or product endorsement purposes.

## REFERENCES

- [1] Dunn, D., Cragolino, G., and Sridhar, N., 2000. In *Scientific Basis for Nuclear Waste Management XXIII*, Materials Research Society, Warrendale, PA, **608**, pp. 89.
- [2] Gordon, G.M., Oct. 2002, *Corrosion Journal*, p. 811.
- [3] Manning, P., and Schöbel, J, 1986. *Werkstoffe und Korrosion*, **37**, pp. 137.
- [4] Asphahani, I., 1989. *The Arabian Journal for Science and Engineering*, **14**, No.2, pp. 317.
- [5] Rebak, R., 1998. In *Passivity and Localized Corrosion*, The Electrochemical Society, Pennington, NJ, **97-26**, pp. 1001.
- [6] Rebak, R., and Koon, N., 1998. *Corrosion/98*, NACE International, Houston, TX, Paper 153.
- [7] Gruss, K., Cragolino, G., Dunn, D., and Sridhar, N., 1998. *Corrosion/98*, NACE International, Houston, TX, Paper 149.
- [8] Rebak, R.B. and Crook, P., 1999. In *Critical Factors in Localized Corrosion III*, The Electrochemical Society, Pennington, NJ, **98-17**, pp. 289.
- [9] Cieslak, M.J., Headley, T.J., and Romig, A.D., 1986. *Metallurgical Transactions A*, **17A**, pp. 2035.
- [10] Rebak, R.B., and Crook, P., 2002. In *Transportation, Storage, and Disposal of Radioactive Materials*, ASME International, New York, NY, **PVP-449**, pp. 111.
- [11] Haynes International, 1997. *Hastelloy C-22 Alloy*. Kokomo, Indiana, pp. 16.
- [12] Pan, Y-M, Dunn, D.S. and Cragolino, G.A.: *Metall. Mater. Trans. A*, 2005, **36A**, pp.1143.
- [13] El-Dasher, B.S., and Torres, S.G.: *Pressure Vessel and Piping Conference 2005*, ASME International, New York, NY, Paper No. PVP-2005-71665. *In Press*
- [14] El-Dasher, B.S., Edgecumbe, T.S., and Torres, S.G., *Metall. Mater. Trans A*, *In press*.
- [15] ASME SFA-5.14, ERNiCrMo-10, ASME International, New York, NY, 2004, sec. II, pp. 325.
- [16] Wright, S.I., and Adams, B.L., 1992. *Metallurgical Transactions A*, **23A**, pp. 759.
- [17] Adams, B.L., Wright, S.I., and Kunze, K., 1993. *Metallurgical Transactions A*, **24A**, pp. 819.



**FIGURE 1-Prism Crevice Assembly (PCA) specimen set up consisting of Alloy 22 specimen, titanium nut, ceramic crevice formers, titanium washers and a titanium bolt. The specimens have a weld seam across the center of the front and back working surfaces.**

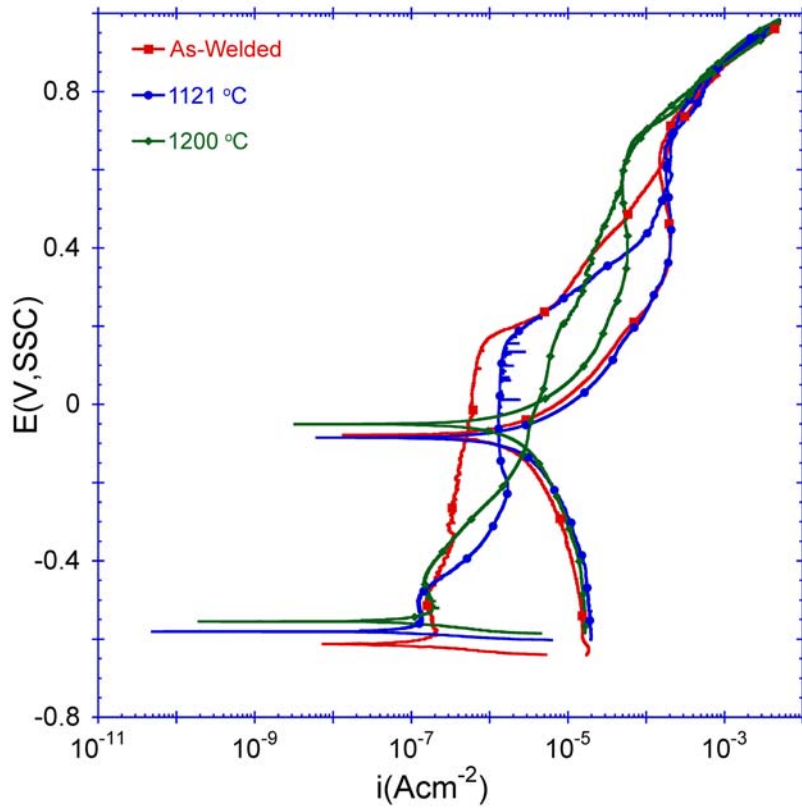
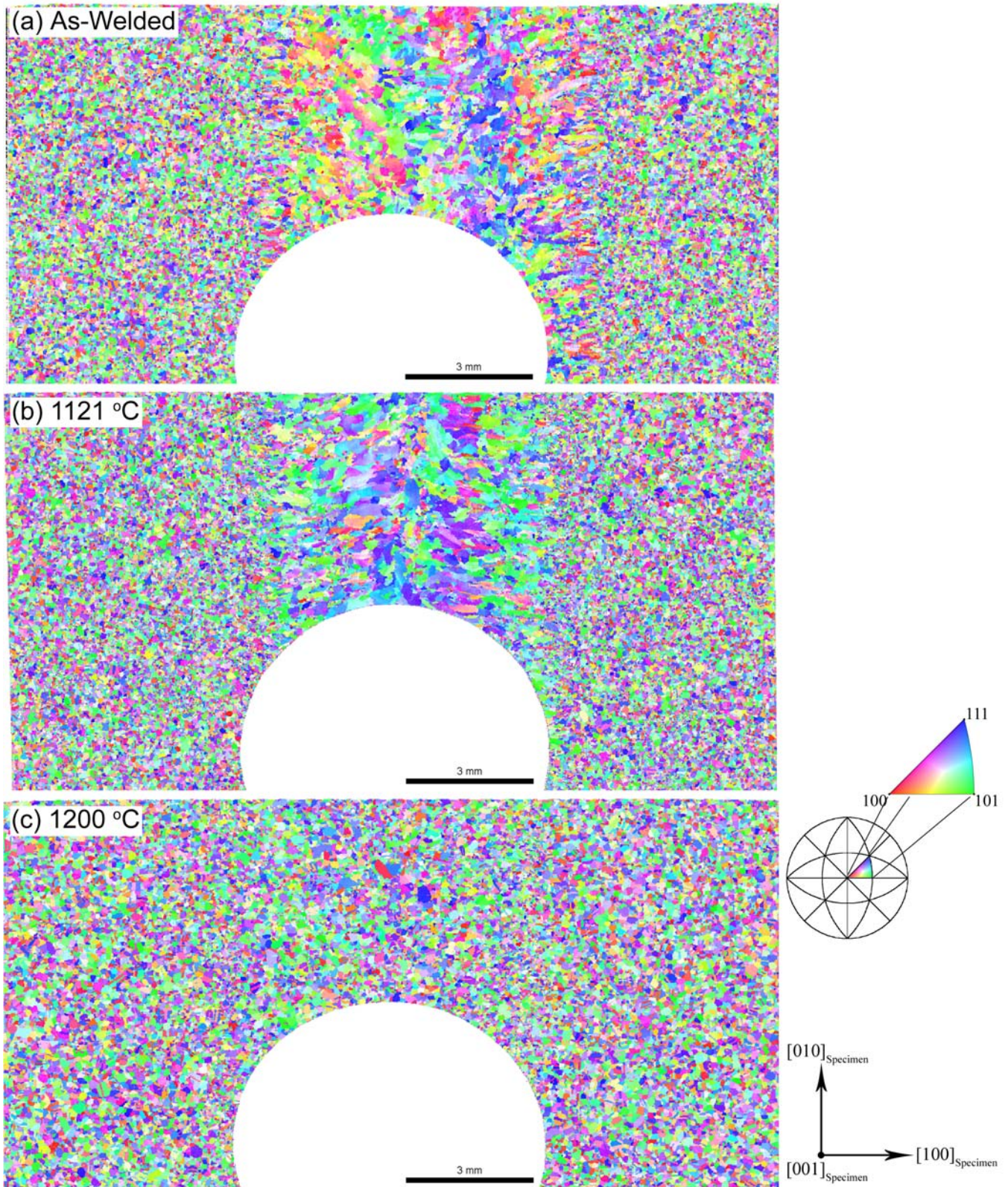
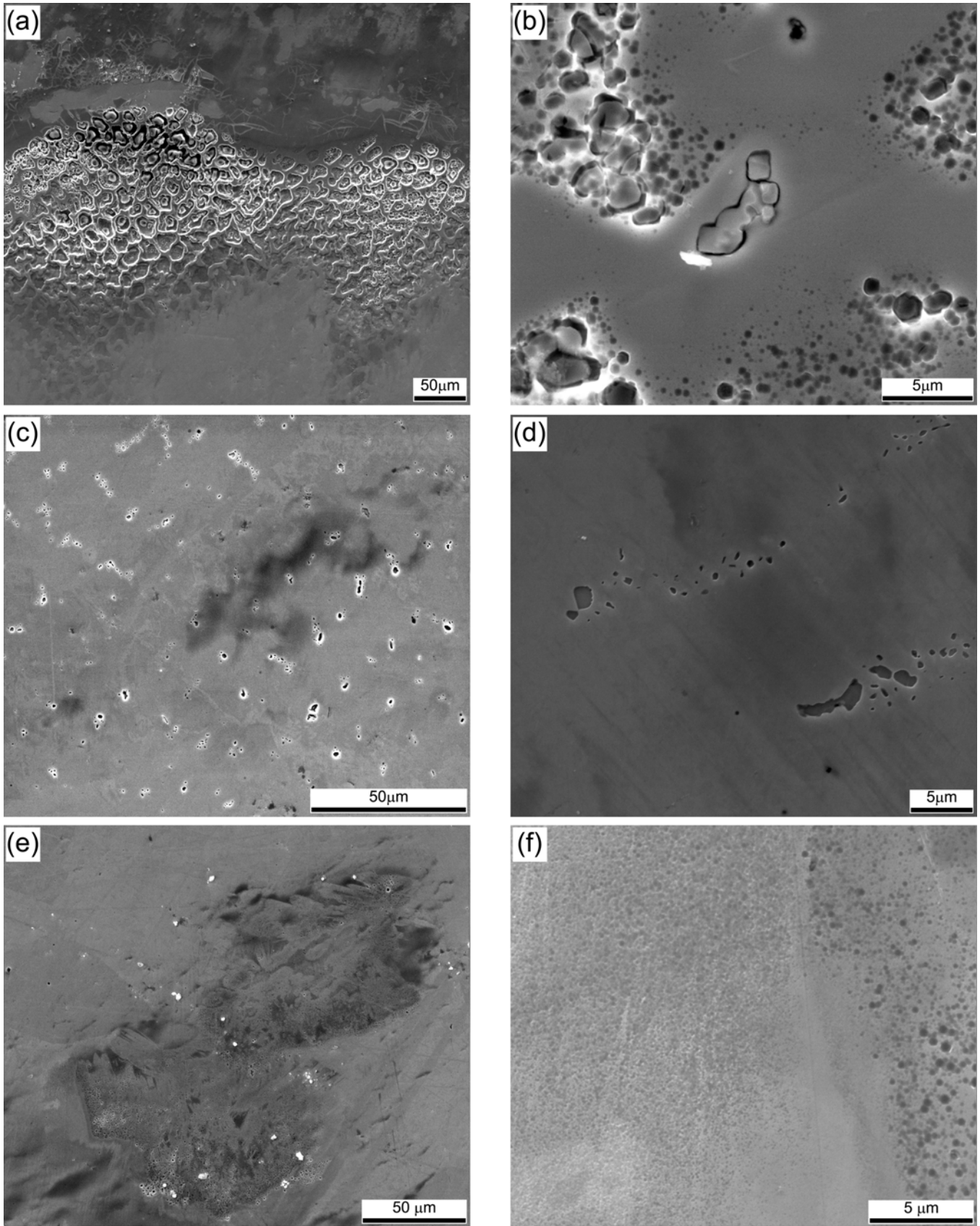


FIGURE 2-Cyclic Polarization curves for the as-welded and solution annealed specimens in 6m NaCl + 0.9m KNO<sub>3</sub> at 90°C.



**FIGURE 3-Inverse Pole Figure maps showing the microstructure of half of one side of the prisms, obtained prior to corrosion testing for the (a) As-Welded specimen, (b) specimen solution annealed at 1121°C for 20 minutes and (c) specimen solution annealed at 1200°C for 20 minutes. Grain colors indicate the crystallographic plane normal parallel to the surface normal.**



**FIGURE 4-SEM Micrographs showing the areas of observed corrosion for: (a) and (b) the as-welded specimen, (c) and (d) the specimen solution annealed for 20 minutes at 1121°C, and (e) and (f) the specimen solution annealed for 20 minutes at 1200°C.**